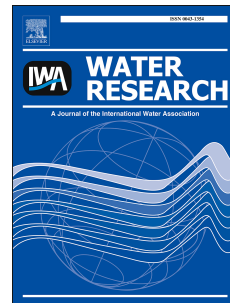


Accepted Manuscript



Evaluating a multi-panel air cathode through electrochemical and biotic tests

Ruggero Rossi, David Jones, Jaewook Myung, Emily Zikmund, Wulin Yang, Yolanda Alvarez Gallego, Deepak Pant, Patrick J. Evans, Martin A. Page, Donald M. Cropek, Bruce E. Logan

PII: S0043-1354(18)30819-4

DOI: [10.1016/j.watres.2018.10.022](https://doi.org/10.1016/j.watres.2018.10.022)

Reference: WR 14133

To appear in: *Water Research*

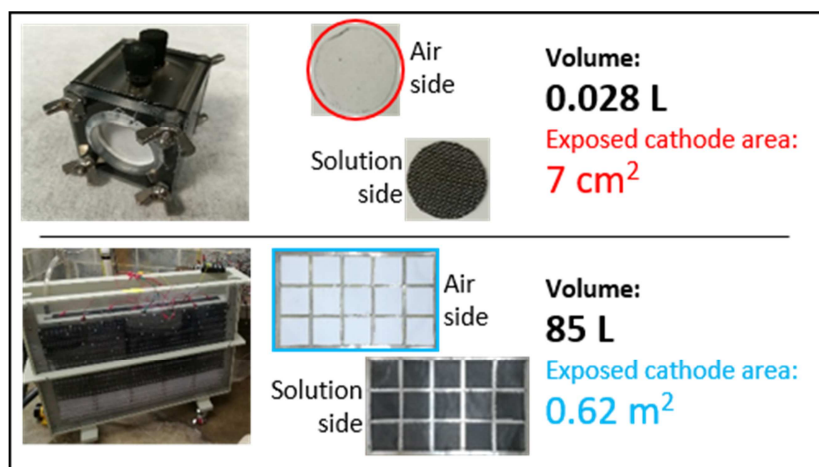
Received Date: 7 August 2018

Revised Date: 4 October 2018

Accepted Date: 7 October 2018

Please cite this article as: Rossi, R., Jones, D., Myung, J., Zikmund, E., Yang, W., Gallego, Y.A., Pant, D., Evans, P.J., Page, M.A., Cropek, D.M., Logan, B.E., Evaluating a multi-panel air cathode through electrochemical and biotic tests, *Water Research* (2018), doi: <https://doi.org/10.1016/j.watres.2018.10.022>.

This is a PDF file of an unedited manuscript that has been accepted for publication. As a service to our customers we are providing this early version of the manuscript. The manuscript will undergo copyediting, typesetting, and review of the resulting proof before it is published in its final form. Please note that during the production process errors may be discovered which could affect the content, and all legal disclaimers that apply to the journal pertain.



Evaluating a multi-panel air cathode through electrochemical and biotic tests

*Ruggero Rossi^a, David Jones^a, Jaewook Myung^b, Emily Zikmund^a, Wulin Yang^a, Yolanda Alvarez Gallego^c, Deepak Pant^c, Patrick J. Evans^d, Martin A. Page^e, Donald M. Cropek^e, and Bruce E. Logan^{*a}*

^a Department of Civil and Environmental Engineering, The Pennsylvania State University, University Park, PA 16802, USA

^b Department of Civil and Environmental Engineering, Southern Methodist University, Dallas, TX 75205, USA

^c Separation & Conversion Technology, Flemish Institute for Technological Research (VITO), Boeretang 200, Mol 2400, Belgium

^d CDM Smith, Bellevue, WA 98007, USA

^e U.S. Army Corps of Engineers, Engineer Research and Development Center, Construction Engineering Research Laboratory, Champaign, IL 61822, USA

*Corresponding author. Tel.: +1 814 863 7908; fax: +1 814 863 7304.
E-mail address: blogan@psu.edu (B.E. Logan).

Abstract

To scale up microbial fuel cells (MFCs), larger cathodes need to be developed that can use air directly, rather than dissolved oxygen, and have good electrochemical performance. A new type of cathode was examined here that uses a “window-pane” approach with fifteen smaller cathodes welded to a single conductive metal sheet to maintain good electrical conductivity across the cathode with an increase in total area. Abiotic electrochemical tests were conducted to evaluate the impact of the cathode size (exposed area of 7 cm², 33 cm², 6200 cm²) on performance for all cathodes having the same active catalyst material. Increasing the size of the exposed area of the electrodes to the electrolyte from 7 cm² to 33 cm² (a single cathode panel) decreased the cathode potential by 5%, and a further increase in size to 6200 cm² using the multi-

31 panel cathode reduced the electrode potential by 55% (at 0.6 A m^{-2}), in a 50 mM phosphate
32 buffer solution (PBS). In 85 L MFC tests with the large cathode using wastewater as a fuel, the
33 maximum power density based on polarization data was $0.083 \pm 0.006 \text{ W m}^{-2}$ using 22 brush
34 anodes to fully cover the cathode, and $0.061 \pm 0.003 \text{ W m}^{-2}$ with 8 brush anodes (40% of
35 cathode projected area) compared to $0.304 \pm 0.009 \text{ W m}^{-2}$ obtained in the 28 mL MFC.
36 Recovering power from large MFCs will therefore be challenging, but several approaches
37 identified in this study can be pursued to maintain performance when increasing the size of the
38 electrodes.

39 **Keywords:** MFC; scaling up; wastewater; chronopotentiometry; air cathode

40

41 **Introduction**

42 Microbial fuel cells (MFCs) have been intensively studied for achieving energy neutral
43 wastewater treatment, or even generating net power production during treatment (Logan and
44 Rabaey, 2012; Logan et al., 2015; Lovley, 2006). Recent advances in MFC reactor architecture
45 and electrode materials have increased energy efficiencies in laboratory scale reactors, and
46 simultaneously lowered material costs (Santoro et al., 2017; Sleutels et al., 2012; Zhang et al.,
47 2014b). However, most MFC studies have used acetate as a substrate rather than actual
48 wastewaters as the fuel, or well-buffered solutions with higher conductivities than those of
49 typical wastewaters, and reactor volumes $<1 \text{ L}$ (Zhang et al., 2013). Small electrode sizes and
50 more favourable test conditions relative to wastewaters, including high substrate concentrations,
51 more conductive solutions, and elevated temperatures ($\sim 30 \text{ }^\circ\text{C}$), can result in performance levels
52 that are much better than those possible using low-strength wastewaters typical at municipal
53 wastewater treatment facilities (He et al., 2016b; Zhang et al., 2013). Although power densities

54 have reached $2.78 \pm 0.08 \text{ W m}^{-2}$ for small MFCs (0.028 L) fed well-buffered phosphate buffer
55 solutions amended with sodium acetate (Rossi et al., 2017), and $0.8 \pm 0.03 \text{ W m}^{-2}$ using domestic
56 wastewater from a primary clarifier (Yang and Logan, 2016), few systems have been examined
57 at reactor sizes of 10 L or more.

58 The main challenges for scaling up MFCs are improving power densities with low-
59 conductivity wastewaters (Fornero et al., 2010; Lanas et al., 2014; Stager et al., 2017), having
60 direct air cathodes rather than dissolved oxygen cathodes, and using inexpensive materials and
61 simple designs for their manufacture (Li et al., 2013). Most of the large-scale MFCs (volume >
62 10 L) to date had two-chamber configurations that use an aqueous catholyte (Dekker et al., 2009;
63 Lu et al., 2017; Vilajeliu-Pons et al., 2017; Wu et al., 2016). One disadvantage of this two-
64 chamber design is that oxygen must be dissolved in the catholyte, which can consume more
65 energy than produced by the MFC in these systems. With air cathodes, oxygen transfer is passive
66 and thus it consumes no energy (Dekker et al., 2009). Another disadvantage is that having a
67 second liquid chamber adds additional ohmic resistance to the system, which will increase the
68 internal resistance and thus lower power production (Liu and Logan, 2004). Power densities for
69 larger-scale MFCs with aerated catholyte systems are low, and in the range of $0.002 - 0.72 \text{ W m}^{-2}$
70 [0.002 W m^{-2} (Lu et al., 2017); 0.67 W m^{-2} (Vilajeliu-Pons et al., 2017); and 0.72 W m^{-2}
71 (Dekker et al., 2009), using an acidified catholyte, pH=4]. Although a high power density of 7.58
72 W m^{-2} (125 W m^{-3}) was recently reported for a two-chamber MFC design (Liang et al., 2018),
73 the values were at least an order of magnitude too large based on conventional methods to report
74 power densities. If the power was normalized by the total of 5 membranes (5 separate circuits) in
75 the module, rather than one membrane area, the maximum power from polarization tests would
76 be 1.52 W m^{-2} . If the total reactor volume was used, rather than a single net anolyte volume, the

77 power density would be 15 W m^{-3} . However, power densities were produced under steady
78 conditions were only 0.085 W m^{-2} (0.98 W m^{-3}). Air cathodes have only been used in a few
79 larger-scale MFCs. In one study, a power density of 0.18 W m^{-2} was obtained with a 90 L MFC
80 treating a brewery wastewater, but individual cathodes had surface areas of only 600 cm^2 (Dong
81 et al., 2015). In another study where a 10000 cm^2 cathode was used, the maximum power density
82 was only 0.058 W m^{-2} , and the design required a thin horizontal flow (flow rate 42 L d^{-1}) to
83 minimize hydrostatic pressure and prevent water leakage (Feng et al., 2014).

84 When scaling up MFCs, the electrode design should be reasonably compact, and allow for
85 easy installation and maintenance (He et al., 2016b; Logan et al., 2015). For a flat plate-and-
86 frame type MFC, the electrode packing density is calculated from the spacing between repeating
87 cathode and anode units. For example, for an anode chamber width of 2 cm (filled with graphite
88 fiber brush anodes) and a cathode chamber width of 2 cm (a 4 cm wide anode-cathode unit), the
89 electrode specific surface area is $25 \text{ m}^2 \text{ m}^{-3}$ (area of the cathode per volume of the reactor)
90 (Logan et al., 2015). Very high electrode packing densities should be avoided to minimize
91 clogging or short circuiting between the electrodes (Li et al., 2013), and the design should allow
92 easy access for maintenance or replacement. One plate-and-frame configuration, called a
93 “cassette” MFC, was made by bolting the anode and cathode together as part of the same cassette
94 (Miyahara et al., 2013; Zhuang et al., 2012). While this allows for good installation and cassette
95 removal, a single electrode cannot be extracted without removing and disassembling the whole
96 cassette. In addition, this design provided only one cathode per anode. More recently, a modular
97 design was developed that used repeating anode and cathode modules, so that anode or cathode
98 modules could be manufactured, installed, and removed without removing the counter electrodes
99 (He et al., 2016a, 2016b). For this specific modular architecture, the anode module was

100 constructed from an array of anode brushes wired together, while a cathode module was formed
101 from two cathodes joined together with an air space between them (He et al., 2016a, 2016b;
102 Logan et al., 2015). These modules were wired so that each anode was connected to two
103 cathodes (one on each side), to improve power production and reduce treatment times.

104 Anode brushes have been frequently used in large scale systems (Cusick et al., 2011; Logan,
105 2010) but not air cathodes. Two challenges for building large air cathodes are the impact of
106 water pressure on cathode performance (Ahn et al., 2014; Cheng et al., 2014a), and increased
107 electrode overpotentials due to reduced electrical conductivities (Cheng et al., 2014b). As the
108 hydraulic pressure on the cathode is increased with the height of the water in the reactor, even if
109 the cathode does not leak, its performance could be reduced due to the high water pressure that
110 reduces the area of the catalyst exposed to the air (Yang et al., 2015). For example, an
111 electrochemical impedance spectroscopy (EIS) analysis of air cathodes showed that the charge
112 transfer resistance increased from 23 Ω to 44 Ω when the water pressure increased from 0.1 m to
113 2 m against the electrode (Cheng et al., 2014a). Electrical conductivities are a major concern
114 during scale up, as electrode dimension gets larger, ohmic resistance increases, because the
115 distance between where electrons are generated and the leading-out terminal where current flows
116 out of anode increases (Cheng et al., 2014b). Even though cathodes are made with relatively
117 conductive carbon materials, there can be substantial power losses due to the electrode
118 overpotentials with the increased size of the electrodes. For example, it was estimated that the
119 electrical power loss could be as much as 47% by increasing the size of a carbon mesh anode
120 from 10 cm² to 1 m² (current density of 3 A m⁻²), based on only one connection to the electrode
121 (Cheng et al., 2014b).

122 In order to obtain large cathodes with good electrical conductivity and performance, we
123 designed and tested a new multi-panel cathode that contained many smaller cathodes welded into
124 a single metal sheet, much like windows are made of many panes of glass (Figure 1) (Patent
125 application no EP17194627). Using a metal sheet provided good electrical connections for all
126 individual cathode panes to the circuit. For the individual panels we used commercially available
127 cathodes with a size of 18 by 18 cm (324 cm²) (Pant et al., 2010; Zhang et al., 2011, 2014a). To
128 evaluate the impact of this design on performance we constructed a cathode containing 15
129 individual cathode panes (3 cathodes high, 5 cathodes wide, 6800 cm² total projected area, 6200
130 cm² exposed area). Performance was examined in an 85 L tank under abiotic conditions using
131 chronoamperometry, and in biotic MFC fed with domestic wastewater. We compared the
132 electrochemical performance of this larger cathode with two smaller cathodes made from a
133 portion of a single cathode pane: 11.3 cm² total projected area square cathodes (7 cm² exposed
134 area) typically used in 0.028 L MFCs (Yang et al., 2017); and larger 52 cm² (33 cm² exposed
135 area) cathodes in a specially designed reactor (0.22 L). Following electrochemical tests, the large
136 multi-paned cathode was examined for power production in an MFC using an anode module with
137 8 or 22 brush anodes, in multiple fed batch tests using domestic wastewater.

138

139 **Materials and methods**

140 *Electrode materials*

141 The cathodes used in electrochemical tests and MFCs were all prepared using sheets (18 by
142 18 cm, 324 cm², 0.45 mm thick) that were manufactured by VITO (Mol, Belgium) using a
143 proprietary process (VITO CORE[®]) based on pressing together a mixture of activated carbon
144 (AC) (70–90 wt%; Norit SX plus, Norit Americas Inc., TX) and polytetrafluoroethylene (PTFE)

145 binder, onto a stainless steel mesh current collector. A PTFE diffusion layer (70% porosity) was
146 then added on top of the catalyst layer which became the air-side of the cathode (Pant et al.,
147 2010). The cathodes for the small (11.3 cm²) and medium (52 cm²) chambers were made from
148 portions cut from these cathode sheets. A circular cathode 3.8 cm in diameter (11.3 cm²) was
149 used for the smallest reactor (0.028 L), and a rectangular cathode of 9.2 cm by 5.6 cm (52 cm²)
150 was used in the middle-sized reactor (0.22 L). The large cathode (107 cm long by 0.64 cm in
151 height, 6800 cm²) was manufactured by VITO based on a specified overall electrode size, and
152 contained 15 cathode sheets that were welded into laser cut holes (“window panes”) in the
153 stainless steel frame to allow the cathode sheets to be exposed to water on one side, and air on
154 the other side (Figure 1). The use of a single metal panel enabled a low resistance of $\leq 0.2 \Omega$
155 between the center of any cathode panel and any part of the external stainless steel panel.

156 Brush anodes were made with two different sizes for the various sized-chamber MFC tests.
157 For the smaller reactor, brushes were 2.5 cm in diameter, and 2.5 cm long, and made from
158 graphite fiber (PANEX 35 50K, Zoltek) wound between two titanium wires (Mill-Rose, Mentor,
159 OH) (Logan et al., 2007; Yang et al., 2017). The brushes used in the larger reactor were 5.1 cm in
160 diameter and 61 cm long, made from the same materials as the smaller brushes (Gordon Brush,
161 CA, USA) (Cusick et al., 2011). All anodes were heat treated at 450 °C in air for 30 min prior to
162 use in MFCs (Feng et al., 2010).

163

164 *Bench and pilot-scale reactors*

165 Three different electrochemical cells were constructed to evaluate the impact of scaling up
166 the cathode size on the electrochemical performance (Figure 1). The small cell (SC) was a single
167 chamber, cube-shaped reactor constructed from a polycarbonate block 4 cm in length (5 cm × 5

168 cm), with an inside cylindrical chamber having a diameter of 3 cm (0.028 L total volume), and
169 an exposed cathode area of 7 cm² that has been used in many previous MFC laboratory studies
170 (Figure 1C) (Yang et al., 2017). The cathode specific surface area was 25 m² m⁻³ anolyte
171 volume.

172 The medium-sized cell (MC) was a polycarbonate rectangular-shaped reactor, with an
173 anolyte chamber 10.9 cm long, 3.5 cm wide, and 6.2 cm high, filled with 0.22 L of electrolyte
174 (Figure 1D, Figure S1). The cell had a bracket slot 3.5 cm from the wall of the water side, where
175 the cathode was attached separating the anolyte chamber from the air cathode chamber. The
176 cathodes were secured to the frame with 10 screws using a plastic U-shape fastener and a gasket
177 (butyl rubber). The air chamber was 6.8 cm long, 1.0 cm wide and 4.4 cm high. The cathode
178 specific surface area was 15 m² m⁻³ anolyte volume.

179 The large cell (LC) was a custom rectangular tank (1.1 m long, 0.15 m wide and 0.85 m
180 height) that was used to examine the physical properties of the cathodes, such as mechanical
181 strength (deformation when filled) and the resistance to water pressure (based on leaking), as
182 well as to evaluate the electrochemical characteristics of the cathodes (Figure 1E). The tank had
183 a bracket slot 10 cm from the wall of the water side, where the cathode was attached to form the
184 anolyte chamber. The cathodes were secured to the frame with 25 screws using a plastic U-shape
185 fastener and a gasket (closed cell PVC vinyl foam). The anolyte tank was filled with 85 L of
186 water, and examined by eye for deformation and water leakage when filled. The cathode specific
187 surface area was 7.3 m² m⁻³ anolyte volume. This lower specific area of the cathode was used
188 here in order to accommodate the larger diameter anode brushes and inspecting the condition of
189 the electrodes. The cathode air chamber was formed by sliding a sheet of PVC into a slotted
190 groove 5 cm from the cathode. To reduce the cathode deformation due to the pressure of the

191 water on the cathode, the space between the clear PVC sheet and the cathode was filled with 19
192 spacers (Yang et al., 2012), constructed by rolling polypropylene mesh (XN3110-48P, Industrial
193 Netting, USA) into tubes (4 cm diameter by 1 m long), with the rolled tubes held together using
194 zip ties (Figure S2).

195 To examine actual power generation in the LC, an anode module made of polyvinyl chloride
196 (PVC) was constructed using a linear array of graphite fiber brushes. The PVC module held
197 either 8 or 22 brushes (as indicated), with the ends of the brushes secured at the top and bottom
198 of the module (Figure S3). The brush module was placed parallel to the cathode, in the middle of
199 the anode chamber, producing a distance of 3.5 cm between the edge of the anode brushes and
200 the cathode surface in initial tests (Lanas et al., 2014). The anodes were connected in parallel to
201 the circuit by an external single titanium wire. At the top of the anode module, a clip was used to
202 reduce the bending of the cathode sheet and to secure it in position while improving its electrical
203 connection (Figure S4). For the smaller chamber, the anodes were placed horizontally in the
204 middle of MFC chambers (perpendicular to the cathode) with a distance of 1.4 cm between the
205 edge of the brush and the cathode (Vargas et al., 2013; Yang et al., 2017).

206 To avoid any short circuiting and reduce biofilm growth on the cathode, all reactors were
207 operated during the biotic tests with a separator placed on the cathode (PZ-1212, Contec, USA)
208 (Wei et al., 2013; W. Yang et al., 2017). For the SC, a separator with the same area of the
209 cathode was cut from a 30 cm by 30 cm wipe separator. In the LC, 12 separators were sewn
210 together and cut to the final area, same as the cathode (6800 cm²).

211

212 *Electrochemical cell (abiotic) tests*

213 Electrochemical tests were performed using a potentiostat (VMP3, BioLogic, Knoxville,
214 TN) with the cathode as the working electrode (WE), and a steel mesh as the counter electrode
215 (CE) in the medium and large chamber reactors and Pt mesh as the CE in the small chamber.
216 Electrochemical performance of the cathodes was evaluated using chronopotentiometry (CP)
217 tests in a 50 mM phosphate buffer solution (PBS; Na_2HPO_4 , 4.58 g L^{-1} ; $\text{NaH}_2\text{PO}_4 \cdot \text{H}_2\text{O}$, 2.45 g
218 L^{-1} ; NH_4Cl , 0.31 g L^{-1} ; KCl , 0.13 g L^{-1} ; pH 7.0; conductivity of $\kappa = 6.25 \text{ mS cm}^{-1}$) or sodium
219 chloride amended tap water ($\kappa = 1.45 \pm 0.05 \text{ mS cm}^{-1}$) in the presence or absence of the
220 separator. Current was fixed for 20 min over a range of 0 to -4 mA in the SC, 0 to -10 mA in
221 the MC, and 0 to -0.4 A in the LC. An Ag/AgCl reference electrode (RE - 5B, BASi, West
222 Lafayette, IN; $+0.209 \text{ V vs. SHE}$) was used in the SC and MC electrochemical tests, and placed
223 1.2 cm from the cathode. The ohmic losses due to the distance between the RE and the WE were
224 corrected based on the conductivity of the solution (see information in SI and Figure S5). An
225 immersion reference electrode (AGG, Electrochemical Devices Inc., OH; $+0.199 \text{ V vs. SHE}$)
226 was used in the large chamber and kept attached to the cathode, in the same position for all the
227 tests. All potentials are reported versus SHE.

228

229 *Microbial fuel cell (biotic) tests*

230 Only the small (SC) and the large cells (LC) were used for biotic tests. The anodes in the SC
231 were fully acclimated to wastewater in MFCs for over four months at a fixed external resistance
232 of 1000Ω , at a constant temperature ($30 \text{ }^\circ\text{C}$). Domestic wastewater was collected once a week
233 from the effluent of the primary clarifier at the Pennsylvania State University Wastewater
234 Treatment Plant, and stored at $4 \text{ }^\circ\text{C}$ prior to use. Total and soluble COD were measured using
235 method 5220 (Hach COD system, Hach Company, Loveland, Colorado). Single cycle

236 polarization tests were conducted by varying the external resistance from 1000, 500, 200, 100
237 and 75 Ω at a 20 min interval after open circuiting for 2 h with a total test duration of 3.7 h, in a
238 constant temperature room (30 °C).

239 The LC was operated at room temperature in a laboratory at the Pennsylvania State
240 University Wastewater Treatment Plant in order to feed it directly with fresh primary effluent
241 wastewater (WW). During acclimation of the anodes for the first week of operation, the feed
242 solution was 35 L of primary effluent wastewater mixed with 40 L of 0.5 g L⁻¹ sodium acetate in
243 50 mM PBS, and 10 L effluent collected over several weeks from MFCs fed acetate and
244 wastewater. The external resistance was 1000 Ω for the first two days and then was decreased
245 daily to 100 Ω , 25 Ω , 10 Ω and 5 Ω over the following four days. For the second week of
246 acclimation, the solution was 55 L of wastewater, 20 L of 50 mM PBS containing 0.5 g L⁻¹
247 sodium acetate, and 10 L of MFC effluent. Thereafter, the LC was operated using only primary
248 effluent wastewater. After a stable potential production for three successive fed-batch cycles,
249 single cycle polarization tests were conducted on the LC by feeding the reactor with fresh
250 wastewater and holding the system at open circuit conditions for 2 h, and then varying the
251 external resistance from 100, 25, 10, 5, 2, 1 to 0.4 Ω at 20 min intervals.

252 The current was calculated based on the voltage drop (U) across the external resistor, and
253 recorded using a computer based data acquisition system (2700, Keithley Instrument, OH).
254 Current densities (i) and power densities (P) were normalized to the total exposed cathode area
255 (large chamber area, $A_{LC} = 6200 \text{ cm}^2$, and power P_{LC} ; small chamber area, $A_{SC} = 7 \text{ cm}^2$, and
256 power P_{SC}), and calculated as $i = U/RA$ and $P = iU$, where R is the external resistance and A is
257 the cathode projected area. During each polarization test, anode and cathode potentials were also
258 recorded using a reference electrode. An Ag/AgCl reference electrode (RE-5B, BASi, West

259 Lafayette, IN; + 0.209 V vs. SHE) was used to measure the anode potential (E_{An}) in the SC biotic
260 tests at a distance of 1.2 cm from the cathode. The cathode potential (E_{Ct}) was calculated from
261 the anode potential and the cell potential as $E_{Ct} = U + E_{An}$, and then corrected based on the
262 conductivity of the solution and the distance from the RE (Logan et al., 2018) (SI and Figure S5).
263 An immersion reference electrode (AGG, Electrochemical Devices Inc., OH; + 0.199 V vs. SHE)
264 was used in the LC biotic tests to measure the anode potential (E_{An}), and it was kept close to the
265 cathode, and in the same position for all the tests. The anode potential was corrected based on the
266 conductivity of the solution and the distance from the RE. The cathode potential (E_{Ct}) was
267 estimated using the cell potential as $E_{Ct} = U + E_{An}$ (see information in SI and Figure S5). All
268 potentials are reported versus SHE.

269

270 **Results and discussion**

271 *Electrochemical tests*

272 Chronopotentiometry tests on cathodes of different sizes showed differences in performance,
273 with the smaller cathodes producing the lowest overpotentials at the different set current
274 densities (Figure 2A, Figure S5). For example, at $0.61 \pm 0.00 \text{ A m}^{-2}$ the smaller cathode
275 produced $0.35 \pm 0.00 \text{ V}$, which was only 5% higher than the potential produced by the middle-
276 sized cathode ($0.33 \pm 0.00 \text{ V}$ at $0.62 \pm 0.01 \text{ A m}^{-2}$) but 121% higher than that obtained with the
277 large cathode ($0.16 \pm 0.03 \text{ V}$ at $0.64 \pm 0.00 \text{ A m}^{-2}$). The adverse impact of the increased size of
278 an electrode on performance was consistent with previous studies that showed a loss in power as
279 cathode sizes were increased (Cheng et al., 2014b; Dewan et al., 2008).

280 Chronopotentiometry tests were conducted on the different size cathodes in tap water
281 amended with sodium chloride ($\kappa = 1.45 \pm 0.05 \text{ mS cm}^{-1}$), to evaluate performance in an

282 unbuffered solution with a conductivity similar to that of domestic wastewater (Figure 2B). The
283 overpotentials of all cathodes were larger in the less conductive solution, with the large cathode
284 having much higher overpotentials with respect to the other two cathodes at a given current
285 density. For example, at a current density of $0.64 \pm 0.00 \text{ A m}^{-2}$ the large cathode potential was
286 $0.09 \pm 0.01 \text{ V}$, which was much lower than that of $0.23 \pm 0.00 \text{ V}$ of the medium size cathode
287 ($0.63 \pm 0.00 \text{ A m}^{-2}$) and $0.26 \pm 0.01 \text{ V}$ ($0.62 \pm 0.00 \text{ A m}^{-2}$) for the smaller cathode.

288 Additional chronoamperometry tests were conducted using the large cell to evaluate the
289 impact of the presence of the separator on the electrochemical performance of the cathode over a
290 current density range relevant to operation of the large MFC using wastewater (Figure S6A). The
291 presence of the extra layer of the separator reduced the potential output at 0.64 A m^{-2} from 0.16
292 $\pm 0.03 \text{ V}$ to $0.13 \pm 0.01 \text{ V}$ in PBS, and from $0.09 \pm 0.01 \text{ V}$ to $0.06 \pm 0.00 \text{ V}$ in a low conductivity
293 solution. Insufficient airflow in the cathode chamber could reduce oxygen availability and, thus,
294 cathode performance (Yang et al., 2012). Therefore, an additional electrochemical test was
295 conducted by blowing air into the bottom of the air chamber at 0.5 L min^{-1} (Figure S6B). This
296 airflow across the cathode did not impact the cathode performance, indicating that the size of the
297 air chamber was sufficient to passively provide oxygen transfer to the cathode and that the
298 spacers did not impede passive air flow.

299

300 *Power production of the 85 L MFC fed domestic wastewater (22 anodes)*

301 Following acclimation of the 85 L MFC with the anode module (Figure S3) over three fed-
302 batch cycles, polarization tests were conducted using domestic wastewater (Figure 3). The
303 maximum power density was $0.083 \pm 0.006 \text{ W m}^{-2}$, which was 73% lower than that obtained in
304 the small chamber MFC ($0.304 \pm 0.009 \text{ W m}^{-2}$ in wastewater). The cathode potentials were

305 similar in the abiotic and biotic tests in the 85 L and in the 28 mL reactors (Figure 3A and 3B).
306 There was a significant difference between the open circuit potential (OCP) of the biotic ($0.32 \pm$
307 0.00 V) and abiotic (0.44 ± 0.00 V) tests for the small chamber, but the cathode potentials
308 matched well over the current density range relevant to operation of wastewater fed MFCs. The
309 anode performance was a factor in the reduced power production by the 85 L MFC compared to
310 the 28 mL MFC. For example, after correction for the solution resistance, the slope of the
311 trendline from the linearization of the anode potential was $0.29 \Omega \text{ m}^2$ in LC biotic test, 3.6x
312 higher than the $0.08 \Omega \text{ m}^2$ from the SC biotic tests (Figure 3D, Figure S7). However, there was a
313 much larger reduction in the cathode performance (change of $|0.30 \text{ V}|$, from 0.37 ± 0.04 V at
314 OCP to 0.07 ± 0.02 V at $0.46 \pm 0.03 \text{ A m}^{-2}$) compared to that of the anodes (change of $|0.13 \text{ V}|$,
315 from -0.31 ± 0.01 V at OCP to -0.18 ± 0.02 V at $0.46 \pm 0.03 \text{ A m}^{-2}$). This larger difference for
316 the cathode indicated that in this system the cathode was primarily limiting power production.
317 The decrease in the anode performance was likely a result of both increased size of the anodes
318 and the cathode performance. The anodes in the 85 L MFC were much longer, and had a larger
319 diameter, than those in the small MFC, which both could have contributed to higher
320 overpotentials (Cheng et al., 2014b; Dewan et al., 2008). The increase in water pressure could
321 also have decreased the performance of the cathodes, particularly at the bottom of the MFC
322 where the water pressure was the highest, relative to those at the top of the reactor (Cheng et al.,
323 2014a). This change in the cathode performance could have impacted performance of the anodes
324 opposite to the cathode in the bottom of the large reactor. The reduced active area of the cathode
325 due to the metal frame could also have been a factor in reducing electrode performance, as the
326 metal frame accounted for 23% of the exposed projected area of the cathode (Figure 1).

327 Normalizing the power produced by only the active cathode area results in a power density of
328 0.10 W m^{-2} .

329

330 *Power production of the 85 L MFC fed domestic wastewater using 8 anodes*

331 To further examine the impact of the anodes on performance, we conducted tests using 8
332 anodes instead of 22 anodes. Reducing the number of anodes decreased the anodic projected area
333 by 58% (from 6000 cm^2 to 2500 cm^2), but this decreased the maximum power density by only
334 27%, from $0.083 \pm 0.006 \text{ W m}^{-2}$ to $0.061 \pm 0.003 \text{ W m}^{-2}$ based on the cathode projected area
335 (Figure 4). Power normalized to the projected anode area was $0.152 \pm 0.009 \text{ W m}^{-2}$, which is
336 consistent with previous results showing that using two electrodes with different projected areas
337 improves the relative performance of the smaller (He et al., 2016a; Oh and Logan, 2006).
338 Reducing the number of anodes resulted in slightly increased anode overpotentials. For example,
339 the anode potential at the maximum power density was $-0.177 \pm 0.002 \text{ V}$ at $0.206 \pm 0.006 \text{ A m}^{-2}$
340 (normalized to the projected cathode area) compared to $-0.23 \pm 0.01 \text{ V}$ at the highest current
341 density of $0.250 \pm 0.006 \text{ A m}^{-2}$ with 22 anodes. Thus, maximizing full coverage of the cathodes
342 by the anodes is needed to improve power production (Lanas and Logan, 2013).

343

344 *Impact of the operation time on the MFC performance*

345 Following polarization tests with the 8 anodes, the impact of cathode fouling was examined
346 by comparing the maximum power densities with the existing cathode, which had been operated
347 for 1 month, to the same cathode that was cleaned to remove the surface biofilm, or to a new
348 cathode. The maximum power density increased to 0.057 W m^{-2} after removing the biofilm,
349 which was 36% higher than that obtained prior to biofilm cleaning (0.042 W m^{-2}) (Figure 5).

350 When a new cathode was used, the maximum power density was 0.064 W m^{-2} , which was
351 essentially the same as that originally obtained at the start of the experiments with 8 anodes.

352 The maximum power density decreased by 34% after one month of operation, with 23% due
353 to biofilm formation on the solution side of the cathode, and the remaining 11% due to a
354 combination of the precipitation of salts (An et al., 2017) and the adsorption of organic matter in
355 the wastewater such as humic acids (Yang et al., 2016) and metabolic by-products such as
356 extracellular polymers (Liu et al., 2018). This decrease is only slightly lower than the 39%
357 decrease in the performance previously reported for small chamber MFCs (28 mL volume, 7 cm^2
358 exposed cathode area) after one month of operation (Rossi et al., 2018). This fouled smaller
359 cathode was shown to be successfully cleaned by soaking in a weakly acidic solution for several
360 hours (Rossi et al., 2017; Zhang et al., 2014a), but this approach might not be practical for larger
361 cathodes. We are currently investigating easier ways to clean fouled cathodes. No corrosion of
362 the stainless steel structure was observed after one month of operation.

363 The decline in the cathode potentials further demonstrated that the main reason for the
364 reduced performance of the MFC after one month of operation was the cathode performance. For
365 example, at the maximum power density the potential of the new cathode was 0.19 V (at 0.212 A
366 m^{-2}), compared to 0.07 V (at 0.171 A m^{-2}) for the used cathode. After scraping off the biofilm
367 from the solution side of the fouled cathode, the electrode potential reached 0.16 V (0.200 A m^{-2})
368 at the maximum power density, which was an overall decrease of 11% compared to the new
369 cathode.

370

371 *Treatment performance based on COD removal*

372 The MFC with 8 or 22 anodes achieved similar COD removal efficiencies of 75–80%. The
373 presence of a higher number of anodes therefore did not increase the rate of COD removal,
374 although the number of anodes did impact the amount of COD converted to electricity. The total
375 COD decreased from $428 \pm 12 \text{ mg L}^{-1}$ to $88 \pm 4 \text{ mg L}^{-1}$ after 9 days in the 8 anode configuration.
376 With 22 anodes the COD decreased from $376 \pm 4 \text{ mg L}^{-1}$ to $90 \pm 5 \text{ mg L}^{-1}$ in 11 days. The longer
377 time needed to reduce the COD with 22 anodes was likely due to the higher oxygen content in
378 the 8 anode configuration that might have increased the COD removal rate. The coulombic
379 efficiency (Logan et al., 2006) (CE) was 27% when using 22 anodes, but it decreased to 13%
380 with 8 anodes. The CE obtained here is essentially the same as the 22% previously achieved in
381 small chamber MFC for domestic wastewater at low external resistance (100Ω) (Zhang et al.,
382 2015).

383

384 *Approaches to improve electrochemical performance*

385 Increasing the sizes of the anodes and cathodes resulted in a decrease in the electrode
386 performance despite maintaining the same catalyst and reactor configuration. The greatest impact
387 on performance was due to the cathode. The power density of the large MFC was about one
388 order of magnitude lower than that obtained in the small MFC ($0.083 \pm 0.006 \text{ W m}^{-2}$ vs $0.304 \pm$
389 0.009 W m^{-2}). Fortunately, there are a number of changes in the reactor or electrode design
390 which could be made to improve performance.

391 It should be possible to further improve performance in the large MFC by connecting the
392 anode arrays to two cathodes rather than one cathode, as done in this study. The test chamber
393 used here was designed primarily to test hydraulic stability and electrochemical performance of
394 an abiotic cathode, and thus it was only possible to connect an array of anodes to a single

395 cathode. However, we have previously demonstrated that connecting an anode array with two
396 cathodes, one on either side of the anode array, increased the maximum power density by 62% in
397 fed-batch MFCs (Cheng and Logan, 2011), and by 39–53% for MFCs operated in continuous
398 flow with a feed of domestic wastewater (Kim et al., 2015).

399 It might be possible to improve performance by changing the diameter or the fiber density of
400 the brush anodes. For the tests conducted here, we used anodes with a diameter of 5.1 cm due to
401 their availability from a previous MEC reactor design (Cusick et al., 2011). This larger diameter
402 could have resulted in reduced power due to the average distance of the anode (from the wire
403 core) to the cathode. It was previously shown that reducing 2.5 cm diameter anodes to 0.8 cm
404 improved power, as long as the anode-cathode spacing was not changed. This reduction in size
405 resulted in a 49% increase of the maximum power density (from 0.690 W m^{-2} to 1.030 W m^{-2})
406 using acetate as a substrate in continuous flow MFCs (Stager et al., 2017). However, additional
407 tests with the very small brushes (0.8 cm) with a wastewater feed resulted in unstable MFC
408 performance, while the use of 2.5 cm diameter brushes did not (Stager et al., 2017). Thus, a
409 decrease in brush size from 5.1 cm to 2.5 cm might improve MFC performance without
410 adversely impacting stable power generation, but only if the anode resistance is a substantial part
411 of the overall internal resistance.

412 Reducing the spacing between two deployed electrodes will reduce the ohmic drop and could
413 increase power output, and thus a further reduction in electrode spacing could also improve the
414 performance if the ohmic losses are a main factor in power production (Li et al., 2013). For
415 example, the solution resistance in the large chamber with a 3.5 cm electrode spacing was 0.47
416 Ω , which was 21% of the internal resistance of the reactor (2.19 Ω). Reducing the spacing from

417 3.5 cm to 1.4 cm could further decrease the solution resistance by 60%, to 0.19 Ω , and raise the
418 maximum power density.

419 Increasing the active area of the cathode, and operating with lower hydraulic pressure, could
420 also improve its performance. The stainless steel frame used here reduced the active area of the
421 cathode by 23%, and thus reducing the size of the frame relative to the cathode panels could help
422 improve performance. The hydraulic pressure against the cathode has been shown to reduce the
423 performance of some cathodes, likely due to the increased catalyst flooding with water (Ahn et
424 al., 2014; Cheng et al., 2014a). Further experiments should be conducted on the impact of
425 hydraulic pressure on large scale cathodes by carrying out abiotic tests with different volumes of
426 electrolyte in the chamber. It might be possible to improve the cathode performance by making
427 them more hydrophobic by varying binder content or diffusion layer porosities, or by using a
428 different type of diffusion layer (Yang et al., 2015). It might also be possible to use different
429 cathodes in the bottom of the chamber where the water pressure is greatest, compared to
430 cathodes at the top where water pressure is lower.

431 As previously noted, a critical factor in scaling up MFCs is maintaining sufficient cathode
432 surface area per volume (cathode specific surface area) as the reactor size is increased in order to
433 achieve rapid COD removal and maintain a good volumetric power density (Logan et al., 2015).
434 The cathode specific surface area of the large chamber used in this study was only 7.3 $\text{m}^2 \text{m}^{-3}$,
435 due to the original design factors for evaluating abiotic cathode performance. This is much lower
436 than the 25 $\text{m}^2 \text{m}^{-3}$ previously used in many MFC tests (He et al., 2016b; Logan et al., 2015).
437 Thus, the overall performance in terms of COD removal rate as well as power density will be
438 increased in planned larger scale designs based on closer electrode spacing, and connecting an
439 anode array to two cathodes.

440

441 **Conclusions**

442 A 6200 cm² air-cathode made of fifteen smaller cathodes welded to a single conductive metal
443 sheet was examined in abiotic and biotic tests. Overall, the performance of the large cathode
444 (6200 cm²) decreased relative to the smaller cathodes (7 cm², 33 cm²). However, the maximum
445 power density of $0.083 \pm 0.006 \text{ W m}^{-2}$ was comparable to that obtained in other larger-scale
446 aqueous catholyte MFCs, but there was no catholyte or water aeration needed for our system.
447 Thus, the design provided an energy-positive system due to passive oxygen transfer to the air
448 cathode. Full coverage of the cathode by the brush anodes was needed, as reducing the anode
449 projected area from 6000 cm² to 2500 cm² decreased the maximum power density by 27% to
450 $0.061 \pm 0.003 \text{ W m}^{-2}$. These tests showed the first time that an air cathode could function in a
451 large-scale MFC at a high hydrostatic water pressure (85 cm water height). Several design
452 factors were discussed that could lead to further improvements in overall power production, such
453 as closer electrode spacing and a more hydrophobic diffusion layer with increased water
454 pressures.

455

456 **ASSOCIATED CONTENT**457 **Supporting Information.**

458 Calculations and figures showing the correction for the ohmic drop in abiotic and biotic tests,
459 one figure showing the impact of the separator and the air flow at the bottom of the air chamber
460 on the electrochemical performance of the cathode. Four figures showing the reactor
461 configuration. One table summarizing the results in terms of electrode potential, maximum
462 power density and current density in the MFC with 8 or 22 anode brushes.

463

464 **AUTHOR INFORMATION**465 **Corresponding Author**

466 *E-mail: blogan@psu.edu. Phone: +1-814-863-7908, Fax: +1 814 863-7304.

467

468 **ORCHID**

469 Bruce E. Logan: 0000-0001-7478-8070

470 Ruggero Rossi: 0000-0002-3807-3980

471

472 **Notes**

473 In the event of Vito's fabrication method of the large electrode being commercialised, two
474 authors (Deepak Pant and Yolanda Alvarez Gallego) declare a competing financial interest due
475 to employment at VITO. The other authors have no competing financial interest.

476

477 **ACKNOWLEDGEMENTS**

478 The authors kindly acknowledge Dr. Sara Andreoli and Ms. Katherine Lawson for the
479 preparation of the separators. The research was supported by funds provided by the
480 Environmental Security Technology Certification Program via cooperative research agreement
481 W9132T-16-2-0014 through the US Army Engineer Research and Development Center.

482

483 **References**

- 484 Ahn, Y., Zhang, F., Logan, B.E., 2014. Air humidity and water pressure effects on the
485 performance of air-cathode microbial fuel cell cathodes. *J. Power Sources* 247, 655–659.
486 <https://doi.org/10.1016/j.jpowsour.2013.08.084>
- 487 An, J., Li, N., Wan, L., Zhou, L., Du, Q., Li, T., Wang, X., 2017. Electric field induced salt
488 precipitation into activated carbon air-cathode causes power decay in microbial fuel cells.
489 *Water Res.* 123, 369–377. <https://doi.org/10.1016/j.watres.2017.06.087>
- 490 Cheng, S., Liu, W., Guo, J., Sun, D., Pan, B., Ye, Y., Ding, W., Huang, H., Li, F., 2014a. Effects
491 of hydraulic pressure on the performance of single chamber air-cathode microbial fuel cells.
492 *Biosens. Bioelectron.* 56, 264–270. <https://doi.org/10.1016/j.bios.2014.01.036>
- 493 Cheng, S., Logan, B.E., 2011. Increasing power generation for scaling up single-chamber air
494 cathode microbial fuel cells. *Bioresour. Technol.* 102, 4468–4473.
495 <https://doi.org/10.1016/j.biortech.2010.12.104>
- 496 Cheng, S., Ye, Y., Ding, W., Pan, B., 2014b. Enhancing power generation of scale-up microbial
497 fuel cells by optimizing the leading-out terminal of anode. *J. Power Sources* 248, 631–638.
498 <https://doi.org/10.1016/j.jpowsour.2013.10.014>
- 499 Cusick, R.D., Bryan, B., Parker, D.S., Merrill, M.D., Mehanna, M., Kiely, P.D., Liu, G., Logan,
500 B.E., 2011. Performance of a pilot-scale continuous flow microbial electrolysis cell fed
501 winery wastewater. *Appl. Microbiol. Biotechnol.* 89, 2053–2063.
502 <https://doi.org/10.1007/s00253-011-3130-9>
- 503 Dekker, A., Ter Heijne, A., Saakes, M., Hamelers, H.V.M., Buisman, C.J.N., 2009. Analysis and
504 improvement of a scaled-up and stacked microbial fuel cell. *Environ. Sci. Technol.* 43,
505 9038–9042. <https://doi.org/10.1021/es901939r>
- 506 Dewan, A., Beyenal, H., Lewandowski, Z., 2008. Scaling up Microbial Fuel Cells. *Environ. Sci.*
507 *Technol.* 42, 7643–7648. <https://doi.org/10.1021/Es800775d>
- 508 Dong, Y., Qu, Y., He, W., Du, Y., Liu, J., Han, X., Feng, Y., 2015. A 90-liter stackable baffled

- 509 microbial fuel cell for brewery wastewater treatment based on energy self-sufficient mode.
510 *Bioresour. Technol.* 195, 66–72. <https://doi.org/10.1016/j.biortech.2015.06.026>
- 511 Feng, Y., He, W., Liu, J., Wang, X., Qu, Y., Ren, N., 2014. A horizontal plug flow and stackable
512 pilot microbial fuel cell for municipal wastewater treatment. *Bioresour. Technol.* 156, 132–
513 138. <https://doi.org/10.1016/j.biortech.2013.12.104>
- 514 Feng, Y., Yang, Q., Wang, X., Logan, B.E., 2010. Treatment of carbon fiber brush anodes for
515 improving power generation in air-cathode microbial fuel cells. *J. Power Sources* 195,
516 1841–1844. <https://doi.org/10.1016/j.jpowsour.2009.10.030>
- 517 Fornero, J.J., Rosenbaum, M., Angenent, L.T., 2010. Electric power generation from municipal,
518 food, and animal wastewaters using microbial fuel cells. *Electroanalysis* 22, 832–843.
519 <https://doi.org/10.1002/elan.200980011>
- 520 He, W., Wallack, M.J., Kim, K.Y., Zhang, X., Yang, W., Zhu, X., Feng, Y., Logan, B.E., 2016a.
521 The effect of flow modes and electrode combinations on the performance of a multiple
522 module microbial fuel cell installed at wastewater treatment plant. *Water Res.* 105, 351–
523 360. <https://doi.org/10.1016/j.watres.2016.09.008>
- 524 He, W., Zhang, X., Liu, J., Zhu, X., Feng, Y., Logan, B.E., 2016b. Microbial fuel cells with an
525 integrated spacer and separate anode and cathode modules. *Environ. Sci. Water Res.*
526 *Technol.* 2, 186–195. <https://doi.org/10.1039/c5ew00223k>
- 527 Kim, K.Y., Yang, W., Logan, B.E., 2015. Impact of electrode configurations on retention time
528 and domestic wastewater treatment efficiency using microbial fuel cells. *Water Res.* 80, 41–
529 46. <https://doi.org/10.1016/j.watres.2015.05.021>
- 530 Lanas, V., Ahn, Y., Logan, B.E., 2014. Effects of carbon brush anode size and loading on
531 microbial fuel cell performance in batch and continuous mode. *J. Power Sources* 247, 228–
532 234. <https://doi.org/10.1016/j.jpowsour.2013.08.110>
- 533 Lanas, V., Logan, B.E., 2013. Evaluation of multi-brush anode systems in microbial fuel cells.
534 *Bioresour. Technol.* 148, 379–385. <https://doi.org/10.1016/j.biortech.2013.08.154>
- 535 Li, W.-W., Yu, H.-Q., He, Z., 2013. Towards sustainable wastewater treatment by using
536 microbial fuel cells-centered technologies. *Energy Environ. Sci.* 7, 911–924.
537 <https://doi.org/10.1039/C3EE43106A>
- 538 Liang, P., Duan, R., Jiang, Y., Zhang, X., Qiu, Y., Huang, X., 2018. One-year operation of 1000-
539 L modularized microbial fuel cell for municipal wastewater treatment. *Water Res.* 141, 1–8.
540 <https://doi.org/10.1016/J.WATRES.2018.04.066>
- 541 Liu, H., Logan, B.E., 2004. Electricity generation using an air-cathode single chamber microbial
542 fuel cell in the presence and absence of a proton exchange membrane. *Environ. Sci.*
543 *Technol.* 38, 4040–4046. <https://doi.org/10.1021/es0499344>
- 544 Liu, W., Cheng, S., Yin, L., Sun, Y., Yu, L., 2018. Influence of soluble microbial products on the

- 545 long-term stability of air cathodes in microbial fuel cells. *Electrochim. Acta* 261, 557–564.
546 <https://doi.org/10.1016/j.electacta.2017.12.154>
- 547 Logan, B., Cheng, S., Watson, V., Estadt, G., 2007. Graphite fiber brush anodes for increased
548 power production in air-cathode microbial fuel cells. *Environ. Sci. Technol.* 41, 3341–3346.
549 <https://doi.org/10.1021/es062644y>
- 550 Logan, B.E., 2010. Scaling up microbial fuel cells and other bioelectrochemical systems. *Appl.*
551 *Microbiol. Biotechnol.* 85, 1665–1671. <https://doi.org/10.1007/s00253-009-2378-9>
- 552 Logan, B.E., Hamelers, B., Rozendal, R., Schröder, U., Keller, J., Freguia, S., Aelterman, P.,
553 Verstraete, W., Rabaey, K., 2006. Microbial fuel cells: Methodology and technology.
554 *Environ. Sci. Technol.* 40, 5181–5192. <https://doi.org/10.1021/es0605016>
- 555 Logan, B.E., Rabaey, K., 2012. Conversion of wastes into bioelectricity and chemicals by using
556 microbial electrochemical technologies. *Science* (80-.). 337, 686–690.
557 <https://doi.org/10.1126/science.1217412>
- 558 Logan, B.E., Wallack, M.J., Kim, K.Y., He, W., Feng, Y., Saikaly, P.E., 2015. Assessment of
559 microbial fuel cell configurations and power densities. *Environ. Sci. Technol. Lett.* 2, 206–
560 214. <https://doi.org/10.1021/acs.estlett.5b00180>
- 561 Logan, B.E., Zikmund, E., Yang, W., Rossi, R., Kim, K.-Y., Saikaly, P.E., Zhang, F., 2018.
562 Impact of ohmic resistance on measured electrode potentials and maximum power
563 production in microbial fuel cells. *Environ. Sci. Technol.* 52, 8977–8985.
564 <https://doi.org/10.1021/acs.est.8b02055>
- 565 Lovley, D.R., 2006. Bug juice: Harvesting electricity with microorganisms. *Nat. Rev. Microbiol.*
566 4, 497–508. <https://doi.org/10.1038/nrmicro1442>
- 567 Lu, M., Chen, S., Babanova, S., Phadke, S., Salvacion, M., Mirhosseini, A., Chan, S., Carpenter,
568 K., Cortese, R., Bretschger, O., 2017. Long-term performance of a 20-L continuous flow
569 microbial fuel cell for treatment of brewery wastewater. *J. Power Sources* 356, 274–287.
570 <https://doi.org/10.1016/j.jpowsour.2017.03.132>
- 571 Miyahara, M., Hashimoto, K., Watanabe, K., 2013. Use of cassette-electrode microbial fuel cell
572 for wastewater treatment. *J. Biosci. Bioeng.* 115, 176–181.
573 <https://doi.org/10.1016/j.jbiosc.2012.09.003>
- 574 Oh, S.E., Logan, B.E., 2006. Proton exchange membrane and electrode surface areas as factors
575 that affect power generation in microbial fuel cells. *Appl. Microbiol. Biotechnol.* 70, 162–
576 169. <https://doi.org/10.1007/s00253-005-0066-y>
- 577 Pant, D., Van Bogaert, G., De Smet, M., Diels, L., Vanbroekhoven, K., 2010. Use of novel
578 permeable membrane and air cathodes in acetate microbial fuel cells. *Electrochim. Acta* 55,
579 7710–7716. <https://doi.org/10.1016/j.electacta.2009.11.086>
- 580 Rossi, R., Yang, W., Setti, L., Logan, B.E., 2017. Assessment of a metal–organic framework

- 581 catalyst in air cathode microbial fuel cells over time with different buffers and solutions.
582 *Bioresour. Technol.* 233, 399–405. <https://doi.org/10.1016/j.biortech.2017.02.105>
- 583 Rossi, R., Yang, W., Zikmund, E., Pant, D., Logan, B.E., 2018. In situ biofilm removal from air
584 cathodes in microbial fuel cells treating domestic wastewater. *Bioresour. Technol.* 265,
585 200–206. <https://doi.org/10.1016/j.biortech.2018.06.008>
- 586 Santoro, C., Serov, A., Gokhale, R., Rojas-Carbonell, S., Stariha, L., Gordon, J., Artyushkova,
587 K., Atanassov, P., 2017. A family of Fe-N-C oxygen reduction electrocatalysts for
588 microbial fuel cell (MFC) application: Relationships between surface chemistry and
589 performances. *Appl. Catal. B Environ.* 205, 24–33.
590 <https://doi.org/10.1016/j.apcatb.2016.12.013>
- 591 Sleutels, T.H.J.A., Ter Heijne, A., Buisman, C.J.N., Hamelers, H.V.M., 2012.
592 Bioelectrochemical systems: An outlook for practical applications. *ChemSusChem* 5, 1012–
593 1019. <https://doi.org/10.1002/cssc.201100732>
- 594 Stager, J.L., Zhang, X., Logan, B.E., 2017. Addition of acetate improves stability of power
595 generation using microbial fuel cells treating domestic wastewater. *Bioelectrochemistry*
596 118, 154–160. <https://doi.org/10.1016/j.bioelechem.2017.08.002>
- 597 Vargas, I.T., Albert, I.U., Regan, J.M., 2013. Spatial distribution of bacterial communities on
598 volumetric and planar anodes in single-chamber air-cathode microbial fuel cells.
599 *Biotechnol. Bioeng.* 110, 3059–3062. <https://doi.org/10.1002/bit.24949>
- 600 Vilajeliu-Pons, A., Puig, S., Salcedo-Dávila, I., Balaguer, M.D., Colprim, J., 2017. Long-term
601 assessment of six-stacked scaled-up MFCs treating swine manure with different electrode
602 materials. *Environ. Sci. Water Res. Technol.* 3, 947–959.
603 <https://doi.org/10.1039/c7ew00079k>
- 604 Wei, B., Tokash, J.C., Zhang, F., Kim, Y., Logan, B.E., 2013. Electrochemical analysis of
605 separators used in single-chamber, air-cathode microbial fuel cells. *Electrochim. Acta* 89,
606 45–51. <https://doi.org/10.1016/j.electacta.2012.11.004>
- 607 Wu, S., Li, H., Zhou, X., Liang, P., Zhang, X., Jiang, Y., Huang, X., 2016. A novel pilot-scale
608 stacked microbial fuel cell for efficient electricity generation and wastewater treatment.
609 *Water Res.* 98, 396–403. <https://doi.org/10.1016/j.watres.2016.04.043>
- 610 Yang, Q., Feng, Y., Logan, B.E., 2012. Using cathode spacers to minimize reactor size in air
611 cathode microbial fuel cells. *Bioresour. Technol.* 110, 273–277.
612 <https://doi.org/10.1016/j.biortech.2012.01.121>
- 613 Yang, W., Kim, K.Y., Logan, B.E., 2015. Development of carbon free diffusion layer for
614 activated carbon air cathode of microbial fuel cells. *Bioresour. Technol.* 197, 318–322.
615 <https://doi.org/10.1016/j.biortech.2015.08.119>
- 616 Yang, W., Kim, K.Y., Saikaly, P.E., Logan, B.E., 2017. The impact of new cathode materials
617 relative to baseline performance of microbial fuel cells all with the same architecture and

- 618 solution chemistry. *Energy Environ. Sci.* 10, 1025–1033.
619 <https://doi.org/10.1039/c7ee00910k>
- 620 Yang, W., Logan, B.E., 2016. Immobilization of a metal-nitrogen-carbon catalyst on activated
621 carbon with enhanced cathode performance in microbial fuel cells. *ChemSusChem* 9, 2226–
622 2232. <https://doi.org/10.1002/cssc.201600573>
- 623 Yang, W., Rossi, R., Tian, Y., Kim, K.-Y., Logan, B.E., 2017. Mitigating external and internal
624 cathode fouling using a polymer bonded separator in microbial fuel cells. *Bioresour.*
625 *Technol.* 249, 1080–1084. <https://doi.org/10.1016/j.biortech.2017.10.109>
- 626 Yang, W., Watson, V.J., Logan, B.E., 2016. Substantial humic acid adsorption to activated
627 carbon air cathodes produces a small reduction in catalytic activity. *Environ. Sci. Technol.*
628 50, 8904–8909. <https://doi.org/10.1021/acs.est.6b00827>
- 629 Zhang, F., Ge, Z., Grimaud, J., Hurst, J., He, Z., 2013. Long-term performance of liter-scale
630 microbial fuel cells treating primary effluent installed in a municipal wastewater treatment
631 facility. *Environ. Sci. Technol.* 47, 4941–4948. <https://doi.org/10.1021/es400631r>
- 632 Zhang, F., Pant, D., Logan, B.E., 2011. Long-term performance of activated carbon air cathodes
633 with different diffusion layer porosities in microbial fuel cells. *Biosens. Bioelectron.* 30,
634 49–55. <https://doi.org/10.1016/j.bios.2011.08.025>
- 635 Zhang, X., He, W., Ren, L., Stager, J., Evans, P.J., Logan, B.E., 2015. COD removal
636 characteristics in air-cathode microbial fuel cells. *Bioresour. Technol.* 176, 23–31.
637 <https://doi.org/10.1016/j.biortech.2014.11.001>
- 638 Zhang, X., Pant, D., Zhang, F., Liu, J., He, W., Logan, B.E., 2014a. Long-term performance of
639 chemically and physically modified activated carbons in air cathodes of microbial fuel cells.
640 *ChemElectroChem* 1, 1859–1866. <https://doi.org/10.1002/celec.201402123>
- 641 Zhang, X., Xia, X., Ivanov, I., Huang, X., Logan, B.E., 2014b. Enhanced activated carbon
642 cathode performance for microbial fuel cell by blending carbon black. *Environ. Sci.*
643 *Technol.* 48, 2075–2081. <https://doi.org/10.1021/es405029y>
- 644 Zhuang, L., Zheng, Y., Zhou, S., Yuan, Y., Yuan, H., Chen, Y., 2012. Scalable microbial fuel
645 cell (MFC) stack for continuous real wastewater treatment. *Bioresour. Technol.* 106, 82–88.
646 <https://doi.org/10.1016/j.biortech.2011.11.019>

647

648 **Figure captions**

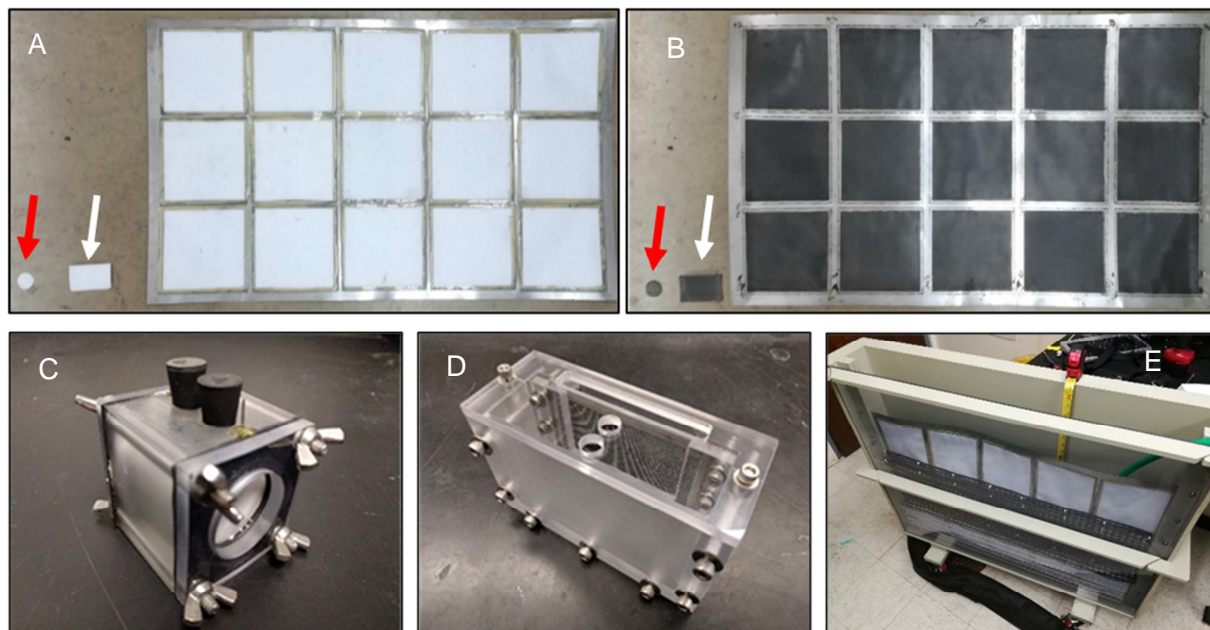
649 **Figure 1.** Photos of the (A) air and (B) solution side of the three cathodes, with sizes (from left
650 to right) of: 11.3 cm² (red arrow), 52 cm² (white arrow) and 6800 cm². (C) Small, (D) medium
651 and (E) large cells used for the electrochemical tests.

652 **Figure 2.** Cathode potential as a function of current density in the abiotic electrochemical cell for
653 the cathodes in the small (SC), medium (MC) and large cells (LC) in (A) 50 mM PBS (6.25 mS
654 cm⁻¹) and (B) tap water amended with NaCl (1.45 ± 0.05 mS cm⁻¹).

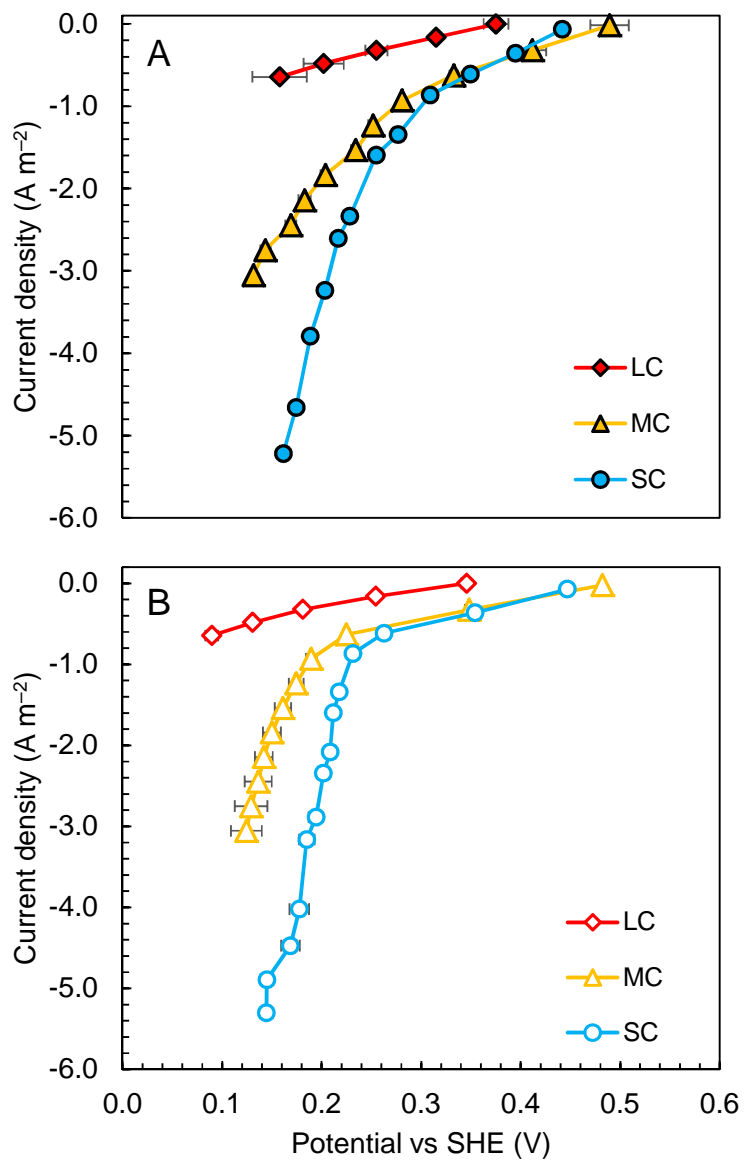
655 **Figure 3.** Cathode (Ct) potentials from the biotic polarization tests and the abiotic
656 chronopotentiometry (CP) in low conductivity solution (LCS) and anode (An) potentials from
657 the biotic polarization tests in the (A) large and (B) small chamber in wastewater (WW). (C)
658 Biotic power density curves in the small chamber (SC) and large chamber (LC) MFC. (D)
659 Comparison of corrected anode potentials in LC and SC.

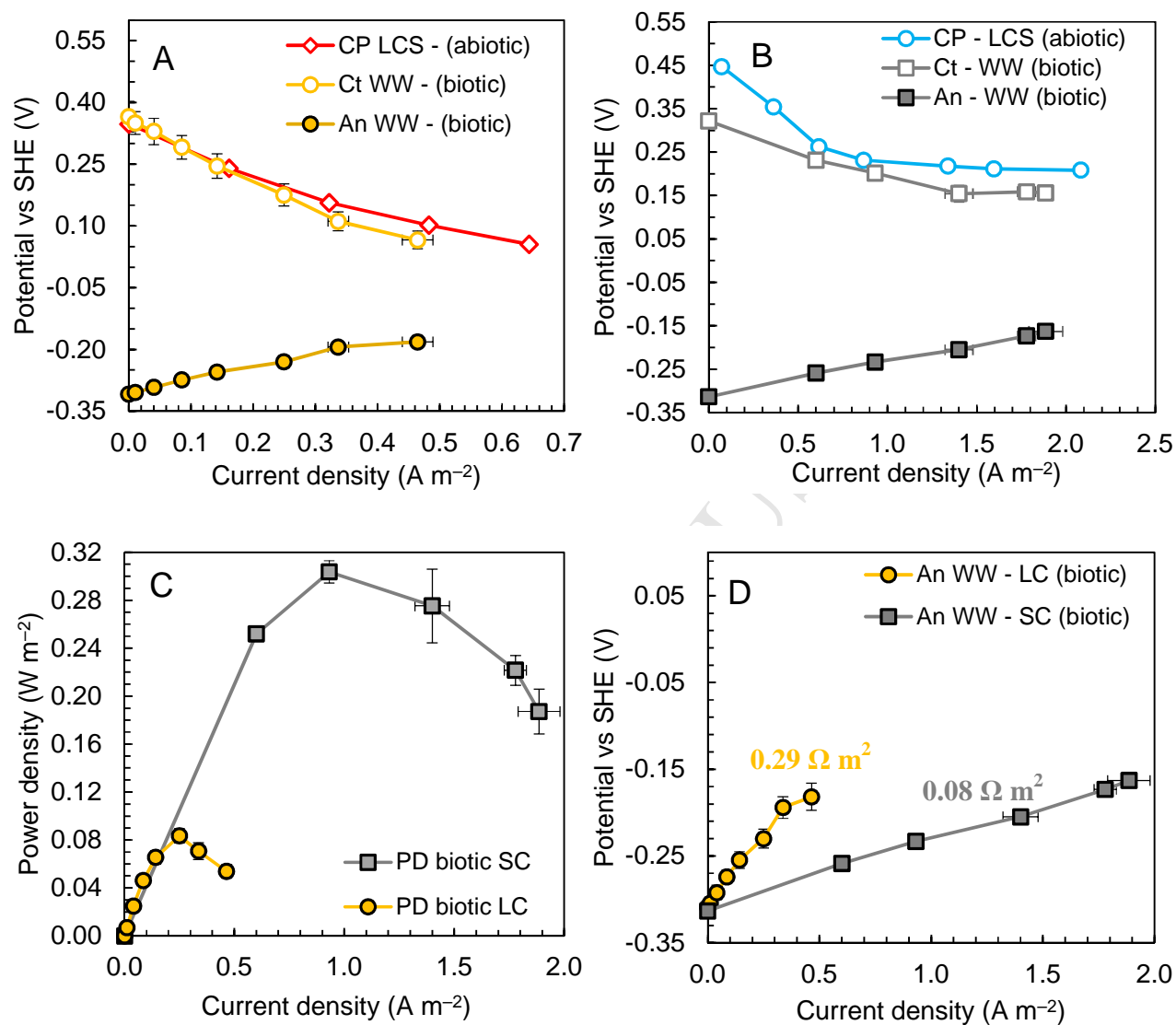
660 **Figure 4.** (A) Cathode potentials (Ct) and anode potentials (An) with an anode module with 8
661 (projected area = 2500 cm²) and 22 anode brushes (projected area = 6000 cm²) compared with
662 the abiotic chronopotentiometry data (CP) and (B) correspondent power density curves.

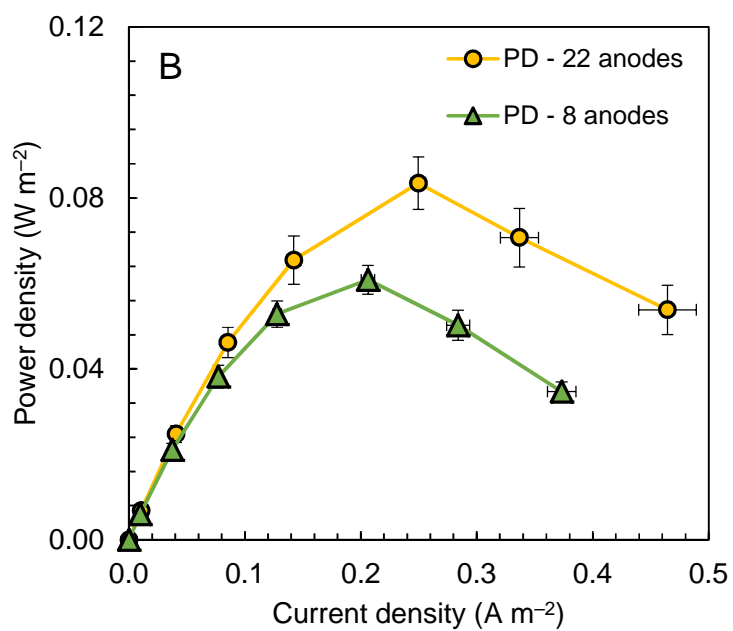
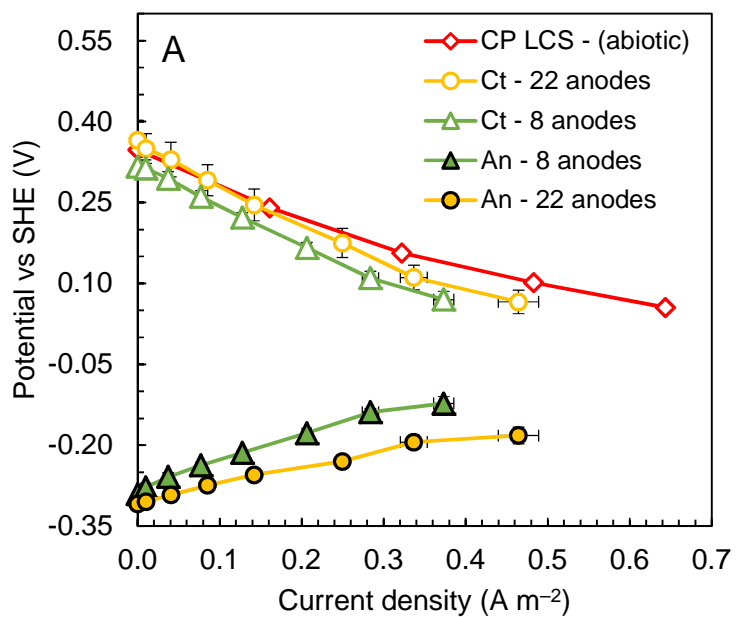
663 **Figure 5.** (A) Cathode potentials (Ct) and anode potentials (An) of the new, cleaned and used (1
664 month) cathode and (B) correspondent power density curves.

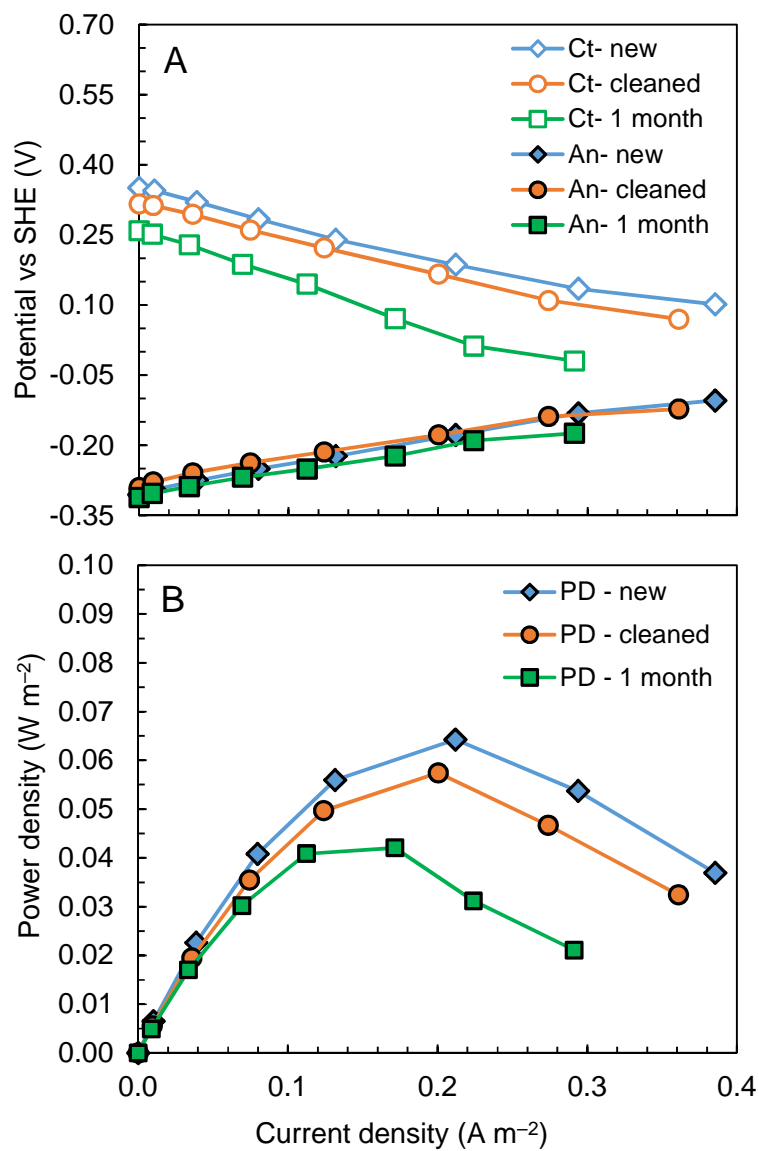


ACCEPTED MANUSCRIPT









Highlights

- Window-pane 0.62 m² cathode successfully installed in 85 L MFC
- The large 15-panel cathode had lower abiotic performance than smaller cathodes
- Power density of $0.083 \pm 0.006 \text{ W m}^{-2}$ was obtained using wastewater as a fuel
- Maintaining full coverage of the electrodes maximized the power production